INTERMEDIARIES FOR GRAVITY-GRADIENT ATTITUDE DYNAMICS II . THE ROLE OF TRIAXIALITY

S. Ferrer[(1)], **F. J. Molero**[(2)], **and F. Crespo**[(3)]
[(1)]*Universidad de Murcia, ES-30071 Espinardo, Spain; +34 868887298, sferrer@um.es*
[(2)]*Universidad de Murcia, ES-30071 Espinardo, Spain; javier.moleromadrid@gmail.com*
[(3)]*Universidad de Murcia, ES-30071 Espinardo, Spain; pacocrespocutillas@gmail.com*

Abstract: *In this paper two Hamiltonian intermediaries $\mathscr{H}_{\{\nu,\phi\}}$ and $\mathscr{H}_{\nu}$ for the gravity-gradient attitude dynamics of a generic triaxial satellite are formulated using Andoyer variables. Assuming the satellite in a circular orbit, both models allow to analyze the coupling between the orbital mean motion and rotational variables and the role played by the moments of inertia in the different types of relative equilibria (families of periodic orbits) defined by each intermediary. The first model $\mathscr{H}_{\{\nu,\phi\}}$ shows that for slow rotation the precession of the angular momentum plane may librate or circulate, connected to a pitchfork bifurcation. Moreover the behavior of the body frame, portrayed by the classic Euler equations, experiences now a switch of stability due to the perturbation defining the model. The study of the second intermediary $\mathscr{H}_{\nu}$ leads to similar expressions, although more cases ought to be discussed due to the fact that two integrals are involved, meanwhile the dynamics features of the angle ϕ are given by a time dependent harmonic oscillator. Our analysis concludes with the comparison of both models taking different moments of inertia and inclinations as initial conditions. The complete integration of these intermediaries and their associates action-angle variables by means of Legendre elliptic integrals are provided elsewhere.*

Keywords: *Attitude dynamics, gravity-gradient, intermediary, relative equilibria, action-angle variables*

1. Introduction

In this paper, the attitude dynamics of a generic triaxial spacecraft in a central gravitational field in Hamiltonian formalism is approached making use of the classic concept of intermediaries in Astrodynamics [1]. The gravity-gradient problem expands since the early days of space dynamics [2] up to the very recent research of spacecraft around asteroids [3]. It covers aspects such as determination, propagation and control, that continue to be areas of research [4, 5]. The problem is formulated in Polar-Nodal and Andoyer variables [1, 6] and we restrict to a satellite in circular orbit. The McCullagh approximation of the potential is assumed and the equations are referred to a rotating system. Following Poincaré and Arnold, we split the Hamiltonian $\mathscr{H} = \mathscr{H}_0 + \mathscr{H}_1$ where $\mathscr{H}_0$ is *an intermediary*, *i.e.* a Hamiltonian function defining a non-degenerate integrable 1-DOF system, which includes the free rigid-body as a particular case. Our approach relies on three main aspects: (i) we abandon the free rigid-body model as the unperturbed system; (ii) we carry out the analysis of the relative equilibria and their bifurcations as functions of the angular momentum which is an integral; (iii) we consider the full set of initial conditions from slow to fast rotations and any inclination among the instantaneous angular momentum plane and the spacial and body frames.

The non-unique way of defining $\mathscr{H}_0$ for the gravity-gradient problem is what asks for a study of the pros and cons of the several possibilities which arise. Indeed, when Andoyer variables are used, some candidates may be considered as intermediaries under the prescription given above; and we do not claim we have made the complete list of them. More precisely, continuing our work on intermediary models [7, 8], after proposing a new one $\mathscr{H}_{\phi}$, we present and compare the main features of two of them.

We study first the flow defined by the intermediary Hamiltonian $\mathscr{H}_{\{\nu,\phi\}}$. Taking advantage of the cyclic character of the Andoyer's variable μ, each value of the angular momentum M leads us to the reduced phase space given by $\mathbb{S}^2_M \times \mathbb{S}^2_M$. Apart from integable, this intermediary is also separable in two subsystems: (ν, N) giving an Euler-type dynamics and (ϕ, Φ), where one of the most remarkable feature is that the node of the angular momentum plane may librate or circulate, connected to a pitchfork bifurcation given for slow rotational motions.

With respect to the second intermediary $\mathscr{H}_{\nu}$, it has received some attention in the past, but in averaged variables and only partially [9, 10]. A first analysis of this intermediary was presented in [8] and the full analysis of relative equilibria (periodic orbits) and their bifurcations will be published elsewhere [11]. One of the main features of this model is that it is endowed with a second axial symmetry related to the angle ϕ. Nevertheless, we do not address the second reduction of this model in order to carry out the comparison of both models at the same level. Moreover, in the case of slow motion, we identify conditions under which the classical unstable equilibria of the free rigid body model switch positions with respect to the principal directions, scenario of great interest in relation to stabilization purposes. Moreover several relative equilibria (or frozen rotations at critical inclinations) are found where the integration reduces to elementary functions.

Both models allow to analyze the coupling between the orbital mean motion and rotational variables, as well as the role played by the moments of inertia in the different types of relative equilibria defined by both intermediaries. Our analysis concludes with the comparison of both models taking different moments of inertia and inclinations as initial conditions. The complete reduction may be carried out by using the Hamilton-Jacobi equation, which gives the action-angle variables defined by each model. The case of $\mathscr{H}_{\nu}$ is an extension of the Sadov's classic set of variables already presented in [8], while the case of $\mathscr{H}_{\{\nu,\phi\}}$ is still in progress. A further analysis is underway in order to look for a scheme, either successive approximations or Lie transforms, with the aim of a compact first order perturbed solutions of the problem.

2. Hamiltonian formulation and intermediaries

We are interested in the roto-translatory dynamics of two bodies, under gravity-gradient interaction, when the main body is assumed to be an sphere; in other words we focus on the dynamics of the second body, being an asteroid, satellite, etc. Moreover, the distance between both bodies is supposed to be such that the potential expansion can be truncated considering the MacCullagh approximation. Then, denoting by T_O, T_R the orbital and rotational kinetic energies and $\mathscr{P}$ the potential, the Hamiltonian function is given by

$$\begin{aligned}\mathscr{H} &= T_O + T_R + \mathscr{P} \\ &= T_O + T_R - \frac{\mathscr{G}M_\odot}{r} + V \\ &= \mathscr{H}_K + \mathscr{H}_R + V, \end{aligned} \tag{1}$$

in other words, the potential is usually split in two parts: a term which depends only on $1/r$ and V, called the perturbing potential, depending on the rest of the variables of the problem. As a result of this, we have that $\mathscr{H}_K = T_O - \mathscr{G}M_\odot/r$ is the Keplerian part of the system and $\mathscr{H}_R = T_R$ is referred as the Euler system (or the free rigid body). Using polar-nodal variables [1] and Andoyer (see Fig. 1) variables [12] we have

$$\mathscr{H}_K = \frac{1}{2}\left(R^2 + \frac{\Xi^2}{r^2}\right) - \frac{\mathscr{G}M_\odot}{r}, \qquad \mathscr{H}_R = \frac{1}{2}\left(\frac{\sin^2\nu}{A} + \frac{\cos^2\nu}{B}\right)(M^2 - N^2) + \frac{1}{2C}N^2. \tag{2}$$

where $\mathscr{G}$ is the gravitational constant, $M_\odot$ is the mass of the disturbing body, r is the distance between the centers of mass of both bodies and $\{A, B, C\}$ are the three principal moments of inertia with $A < B < C$.

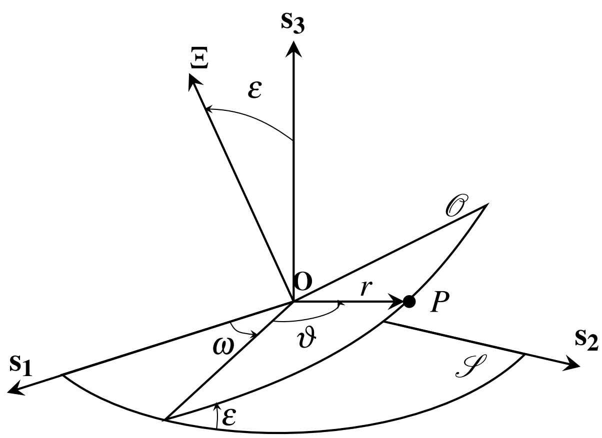

(a) Polar-Nodal variables

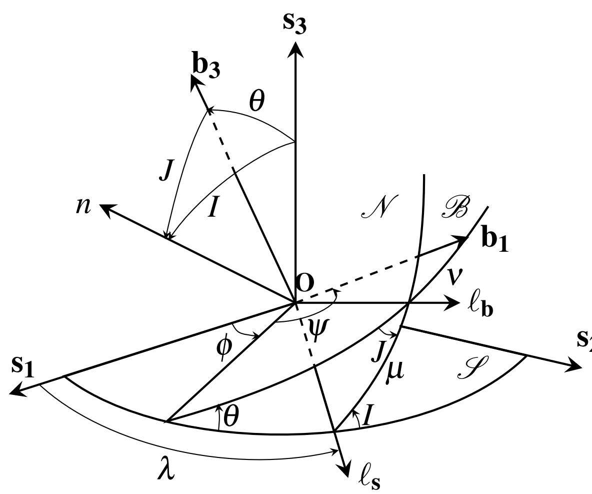

(b) Andoyer variables

Figure 1. Definition of the variables. (a) Polar-nodal variables. (b) Andoyer variables: space $\mathscr{S}$, body $\mathscr{B}$ and nodal $\mathscr{N}$ frames and the angles relating them. Note that the vectors b_2 and $n \times \ell_b$ of the body and nodal frames are not shown in the figure.

2.1. The MacCullagh gravity-gradient disturbing potential

In order to formulate the perturbing potential, we assume that the dimensions of the rigid body are small when compared with the distance to the perturbing body, which allow us to truncate V to the MacCullagh's term [13] given by

$$V = -\frac{\mathscr{G}M_\odot}{2r^3}\left(A + B + C - 3\,\mathscr{D}\right), \tag{3}$$

where

$$\mathscr{D} = A\gamma_1^2 + B\gamma_2^2 + C\gamma_3^2 \tag{4}$$

is the moment of inertia of the rigid body with respect to an axis in the direction of the line joining its center of mass with the perturber, of direction cosines γ_1, γ_2, and γ_3.

By replacing Eq. (4) in Eq. (3) and taking into account that $\gamma_1^2 + \gamma_2^2 + \gamma_3^2 = 1$, we get

$$V = -\frac{\mathscr{G}M_\odot}{2r^3}\left[(C-B)(1-3\gamma_3^2) - (B-A)(1-3\gamma_1^2)\right]. \tag{5}$$

If the orbital plane is chosen as the inertial reference frame, then the orbital reference frame is related to the body frame by the following composition of the rotations:

$$\begin{pmatrix} \gamma_1 \\ \gamma_2 \\ \gamma_3 \end{pmatrix} = R_3(\nu)R_1(J)R_3(\mu)R_1(I)R_3(\phi)\begin{pmatrix} 1 \\ 0 \\ 0 \end{pmatrix} \tag{6}$$

where $\phi = \lambda - \vartheta$ and ϑ is the usual polar coordinate of the orbital motion.

Then, by replacing γ_1 and γ_3 as given by Eq. (6) in the disturbing potential (5), after some calculations we get that,

$$V = -\frac{\mathscr{G}M_\odot}{32r^3}\left[(2C-B-A)V_1 + \frac{3}{2}(B-A)V_2\right]. \tag{7}$$

Thus, this potential V is made of V_1, the "axisymmetric part" given by

$$\begin{aligned} V_1 \;=\;& (4-6s_J^2)\left(2-3s_I^2+3s_I^2C_{2,0,0}\right) \\ & -12s_Jc_Js_I\left[(1-c_I)C_{-2,1,0}+2c_IC_{0,1,0}-(1+c_I)C_{2,1,0}\right] \\ & +3s_J^2\left[(1-c_I)^2C_{-2,2,0}+2s_I^2C_{0,2,0}+(1+c_I)^2C_{2,2,0}\right] \end{aligned} \tag{8}$$

which is independent of ν, and V_2, the "tri-axiality part" given by

$$\begin{aligned} V_2 \;=\;& 6s_I^2s_J^2(C_{2,0,-2}+C_{2,0,2}) - 4(1-3c_I^2)s_J^2C_{0,0,2} \\ & +(1+c_J)^2\left[(1-c_I)^2C_{-2,2,2}+2s_I^2C_{0,2,2}+(1+c_I)^2C_{2,2,2}\right] \\ & +(1-c_J)^2\left[(1-c_I)^2C_{-2,2,-2}+2s_I^2C_{0,2,-2}+(1+c_I)^2C_{2,2,-2}\right] \\ & +4s_Is_J(1+c_J)\left[(1-c_I)C_{-2,1,2}+2c_IC_{0,1,2}-(1+c_I)C_{2,1,2}\right] \\ & -4s_Is_J(1-c_J)\left[(1-c_I)C_{-2,1,-2}+2c_IC_{0,1,-2}-(1+c_I)C_{2,1,-2}\right], \end{aligned} \tag{9}$$

which carries the ν contribution to the perturbation. Note that $C_{i,j,k} \equiv \cos(i\phi + j\mu + k\nu)$ and the notation has been abbreviated by writing $c_I \equiv \cos I$, $s_I \equiv \sin I$, $c_J \equiv \cos J$, and $s_J \equiv \sin J$.

2.2. On the intermediaries

The concept of intermediary is a classic one in astrodynamics (see [1]). In the case of gravity-gradient the basic idea related with them is the definition of an integrable system, that includes part of the potential where the roto-orbital coupling is present. Thus we obtain some advantages, versus the use of the Kepler and free rigid body models, when the perturbation approach is built. In the case the primary is considered to be a sphere, one of the authors has recently proposed a natural intermediary [7]. Here, we continue our work studying some common intermediaries we have identify recently [8]. We have reported on them but for the benefit of the reader, we bring them here again, adding a new one to the previous list.

Note we have listed five intermediaries, but a close look shows they belong to three categories. Indeed, meanwhile the Hamiltonian $\mathscr{H}_\nu$ and $\mathscr{H}_{\{\nu,\phi\}}$ relate to the generic triaxial case, the other pair $\mathscr{H}_\phi$ and $\mathscr{H}_\mu$ fit the almost symmetric bodies; for both pairs we are assuming the satellite in circular orbit and referred to the moving frame. Finally, the one listed first $\mathscr{H}_{\nu,r}$, it seems to be the only integrable case able to give a good approximation when the satellite moves in an elliptic orbit. Details on the dynamical features defined by $\mathscr{H}_{\nu,r}$ are given elsewhere [14].

• **Intermediary 1:** $\mathscr{H}_{\{\nu,r\}}$**.** We consider as a first intermediary the system defined by the following Hamiltonian function

$$\mathscr{H}_{\{\nu,r\}} = \mathscr{H}_K + \mathscr{H}_R + \mathscr{V}$$

where the perturbing potential V_r is a function of the radial distance and two of the rotational momenta. More precisely we have

$$\mathscr{V} \equiv V_r = -\frac{\mathscr{G}M_\odot}{8r^3}(2C-B-A)\left(1-3\frac{\Lambda^2}{M^2}\right). \tag{10}$$

Some readers might argue that it is still integrable the previous Hamiltonian if we add a new term defined by the contribution of 2ϕ, namely

$$\mathscr{V} \equiv V_{\{r,\phi\}} = -\frac{\mathscr{G}M_\odot}{8r^3}(2C-B-A)[2-3s_I^2(1-\cos 2\phi)]. \tag{11}$$

For details on the dynamics of these systems, see [15].

In many applications we may assume the orbit to be circular; then, the radius is constant $r = a$. As a consequence we simplify the previous expressions introducing n, the mean orbital motion, and we will write

$$\mathscr{G}M_\odot = n^2 a^3. \tag{12}$$

As a consequence we will drop from the Hamiltonian the Keplerian term and we will not consider the equations of the system related to the orbital part.

• **Intermediary 2:** $\mathscr{H}_{\{\nu,\phi\}}$**.** Assuming a circular orbit for the satellite, we consider as another intermediary the system whose rotational dynamics defined by the following Hamiltonian function

$$\mathscr{H}_{\{\nu,\phi\}} = \mathscr{H}_R + V_{\{\nu,\phi\}}(\phi,-,\nu,\Phi,M,N) \tag{13}$$

where the potential $V_{\{\nu,\phi\}}$ is now a function of the variables ν and ϕ together with the three rotational moments. We will see below that $\Phi = \Lambda$. More precisely

$$V_{\{\nu,\phi\}} = -\frac{n^2}{8}\left\{(2C-B-A)[(2-3s_I^2+3s_I^2\cos 2\phi)-3s_J^2]-\frac{3}{2}(B-A)s_J^2\cos 2\nu\right\} \qquad (14)$$

and n is again the constant orbital mean motion given in (12). We devote Section 4. to this intermediary. For further details see Crespo[14].

• **Intermediary 3: $\mathscr{H}_\nu$.** Assuming again a circular orbit for the satellite, we consider now as a third intermediary (studied in [8]) the system defined by the following Hamiltonian function

$$\mathscr{H}_\nu = \mathscr{H}_R + V_\nu(-,-,\nu,\Phi,M,N), \qquad (15)$$

where the potential V_ν is a function of the variable ν and three rotational moments, namely

$$V_\nu = -\frac{n^2}{32}\left\{(2C-B-A)(4-6s_J^2)(2-3s_I^2)+\frac{3}{2}(B-A)[-4(1-3c_I^2)s_J^2\cos 2\nu]\right\}. \qquad (16)$$

Note that, with respect to V_ν, the perturbation $V_{\{\nu,\phi\}}$ does not include the secular term $18(2C-B-A)s_I^2 s_J^2$ coming from the axisymmetric part of the potential, which is one of the most important differences between these two intermediaries.

On the other hand, considering quasi-symmetric bodies, as an alternative to the classic expression of the rotational kinetic energy, since the time of Andoyer the function $\mathscr{H}_R$ used to be rearranged as follows

$$\mathscr{H}_R = \frac{1}{4}\left(\frac{1}{A}+\frac{1}{B}\right)(M^2-N^2)+\frac{1}{2C}N^2-\frac{1}{4}\left(\frac{1}{A}-\frac{1}{B}\right)(M^2-N^2)\cos 2\nu, \qquad (17)$$

including the last term as part of the perturbation.

With this in mind, we may consider again a reordering of the gravity-gradient perturbation (7) leading to two intermediaries for quasi symmetric bodies:

• **Intermediary 4: $\mathscr{H}_\phi$.**

$$\begin{aligned}\mathscr{H}_\phi &= \frac{1}{4}\left(\frac{1}{A}+\frac{1}{B}\right)(M^2-N^2)+\frac{1}{2C}N^2 \\ &\quad -\frac{n^2}{16}(2C-B-A)[(4-6s_J^2)\left(2-3s_I^2+3s_I^2\cos 2\phi\right)].\end{aligned} \qquad (18)$$

• **Intermediary 5: $\mathscr{H}_\mu$.**

$$\begin{aligned}\mathscr{H}_\mu &= \frac{1}{4}\left(\frac{1}{A}+\frac{1}{B}\right)(M^2-N^2)+\frac{1}{2C}N^2 \\ &\quad -\frac{n^2}{16}(2C-B-A)[(2-3s_J^2)(2-3s_I^2)-12s_Jc_Js_Ic_I\cos\mu+3s_J^2s_I^2\cos 2\mu].\end{aligned} \qquad (19)$$

A similar study to the one done in this paper for the previous quasi-axial intermediaries is in progress. We devote the rest of this paper to the intermediaries (14) and (16).

3. Methodology. Dealing with a Poisson system in a rotating frame

In this paper we pick two of the above intermediaries in order to compare them. Therefore, it is necessary to tackle both studies with the same methodology, here we present to the reader two technical considerations to apply to each intermediary, with the aim that they become ready for the study.

3.1. Rotating frame

Due to the consideration of a circular orbit, the polar coordinate of the orbital motion is given by $\vartheta = \vartheta_0 + nt$ which involves the time in the Hamiltonian formulation. Nevertheless, the explicit appearance of the time can be avoided by moving to a rotating frame at the same rotation rate as the orbital motion. Because of that, the new variable $\phi = \lambda - nt$ (with $\vartheta_0 = 0$) has been introduced, which is the argument of the ascending node of the angular momentum plane with respect to the inertial plane, in a rotating frame with orbital rate $d\vartheta/dt = n$. Indeed, note that as

$$\frac{\mathrm{d}\phi}{\mathrm{d}t} = \frac{\mathrm{d}\lambda}{\mathrm{d}t} - n = \frac{\partial \mathscr{H}}{\partial \Lambda} - n = \frac{\partial}{\partial \Lambda}(\mathscr{H} - n\Lambda), \tag{20}$$

the change of reference frame requires the introduction of the Coriolis term $-n\Lambda$ in the Hamiltonian. The result is a new conservative Hamiltonian $\mathscr{H}$ with $\Phi \equiv \Lambda$ is now the conjugate momenta of ϕ.

3.2. Poisson reduction

Systems having integrals admit simplifications that allow a better understanding of the qualitative description of dynamics. It is, such a system may be expressed in a new set of variables that incorporates the named integrals. This technique is materialized by means of a transformation of the phase space. Symplectic transformations lead to symplectic reduction and the more general case of a Poisson transformation leave us with a Poisson reduction of the system. The use of symmetries and conservation laws leads to reductions, this technique is part of a very active area of research in the branch of the geometric mechanics, which has a long history going back to the founders of classical mechanics, (see [16, 17]). The reader interested in a deeper insight on the subject would find very helpful the book of Ortega and Ratiu [18], where the authors present the state of the art in reduction, treating the regular, optimal and singular case in detail. What the reader will find below is just some practical applications of those concepts.

It is a known fact that Andoyer's variables are not well defined for the whole set of positions of the body plane with respect to the rotational angular momentum plane. For instance, the analysis of 'polar positions' ($N = M$ or $\Phi = M$) is excluded in Andoyer's variables with the previous formulation; in other words, a second Andoyer chart is needed. This is one of the reasons why we find convenient to study the equilibria of our model in the reduced phase space which, for each value of M, is given by $\mathbb{S}^2_M \times \mathbb{S}^2_M$, *i.e.* a cross product of two spheres with the same radius M.

Thus, considering the non-symplectic transformation $\mathscr{T}_M : (\phi, \nu, \Phi, N) \to (M_1, M_2, M_3, G_1, G_2, G_3)$

given by

$$
\begin{aligned}
M_1 &= \sqrt{M^2 - N^2}\sin\nu, & G_1 &= \sqrt{M^2 - \Phi^2}\sin\phi, \\
M_2 &= \sqrt{M^2 - N^2}\cos\nu, & G_2 &= \sqrt{M^2 - \Phi^2}\cos\phi, \\
M_3 &= N, & G_3 &= \Phi,
\end{aligned}
\tag{21}
$$

where

$$
M_1^2 + M_2^2 + M_3^2 = M^2, \qquad G_1^2 + G_2^2 + G_3^2 = M^2. \tag{22}
$$

Then, the system of differential equations associated to $\mathscr{H}(M_i, G_i)$ is a Poisson's map

$$
\dot{x}_i = \sum_{j=1}^{6} \{x_i, x_j\} \frac{\partial \mathscr{H}}{\partial x_j} \tag{23}
$$

where $x = (x_1, x_2, \dots, x_6) = (M_1, M_2, M_3, G_1, G_2, G_3)$ and the Poisson's bracket are given by

$$
\begin{aligned}
&\{x_1, x_2\} = -x_3, \quad \{x_1, x_3\} = x_2, \quad \{x_3, x_2\} = x_1, \\
&\{x_4, x_5\} = -x_6, \quad \{x_4, x_6\} = x_5, \quad \{x_6, x_5\} = x_4,
\end{aligned}
$$

and $\{x_i, x_j\} = 0$ for any other pair of indices i, j.

3.3. An axial symmetry. A second reduction?

The intermediaries that we study in this paper admit the same Poisson reduction, *i.e.*, the same Poisson map (21), applied to the corresponding phase space leading to a new reduced system. Nevertheless, a big difference arises between those intermediaries, the second one, $\mathscr{H}_\nu$, is endowed with two axial symmetries, thus further reduction may be performed in this case. However, we have decided not to study the second reduce space due to the following two reasons. Since our aim is to compare two Hamiltonian systems, they must be defined on the same reduced space. On the other hand, second reduction does not allow us to identify some of the equilibria of the first reduction, that is to say, under certain conditions, intermediary $\mathscr{H}_\nu$ admits four isolated equilibria in the first reduced space, which can not be identified in the second reduction.

It is worth noticing that the approach proposed here may be put *in parallel* with the way of proceeding in orbital dynamics, started by Cushman [19], Deprit [20] and Deprit *et al.* [21] in the eighties, and reaching until today (see, for instance, Palacian *et al.* [22]). Although there are publications in rotational dynamics with this approach, most of them assume axial symmetry (see for instance Hanßmann [23]); in other words, the qualitative study is done after the second reduction.

4. Intermediary $\mathscr{H}_{\{\nu,\phi\}}$

Accomplishing the requirements of the intermediaries, our model breaks the degeneracy of the Kepler-Euler system although the mathematical apparatus does not grow since only Legendre elliptic integrals are still involved. According to Eqs. (13) and (14), the intermediary $\mathscr{H}_{\{\nu,\phi\}}$ in the rotating frame is given by

$$\begin{aligned}\mathscr{H}_{\{\nu,\phi\}} \equiv \mathscr{H}_0^{\{\nu,\phi\}} &= \frac{1}{2}\left(\frac{\sin^2\nu}{A}+\frac{\cos^2\nu}{B}\right)(M^2-N^2)+\frac{N^2}{2C}-n\Phi \\ &-\frac{n^2}{8}\left\{(2C-B-A)[(2-3s_I^2+3s_I^2\cos 2\phi)-3s_J^2]-\frac{3}{2}(B-A)s_J^2\cos 2\nu\right\}.\end{aligned} \tag{24}$$

Note that we have a separable system which defines two 1-DOF subsystems in (ν,N) and (ϕ,Φ) plus a quadrature giving μ. Comparisons with the full model below show that, in the absence of resonances, almost periodic oscillations separate the intermediary from the complete gravity-gradient model Hamiltonian $\mathscr{H}$.

4.1. From Hamiltonian to Poisson dynamics. The reduced flow

Taking into account the symmetry associated to M, making use of the transformation 21, the new reduced Hamiltonian (24) takes the form

$$\mathscr{H}_0^{\{\nu,\phi\}} = \mathscr{H}_M + \mathscr{H}_G, \tag{25}$$

where

$$\mathscr{H}_M = \frac{1}{2}\left(\frac{M_1^2}{A^*}+\frac{M_2^2}{B^*}+\frac{M_3^2}{C^*}\right), \tag{26}$$

with

$$\frac{1}{A^*}=\frac{1}{A}-\frac{3n^2}{8M^2}(B-A), \quad \frac{1}{B^*}=\frac{1}{B}+\frac{3n^2}{8M^2}(B-A), \quad \frac{1}{C^*}=\frac{1}{C}-\frac{3n^2}{4M^2}(2C-B-A) \tag{27}$$

and

$$\mathscr{H}_G = -nG_3+\frac{n^2}{8M^2}(2C-B-A)(M^2+6G_1^2). \tag{28}$$

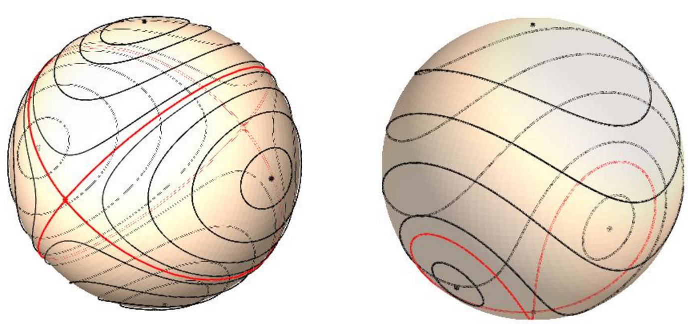

Figure 2. A snapshot of the reduced flow for a small value of M. From left to right we show the intersections of the momentum spheres $\mathbb{S}_M^2$ defining the reduce space with the integral surfaces $\mathscr{H}_M$ and $\mathscr{H}_G$.

Thus, after some computations, the explicit expression of the reduced flow for our system 23 is given by

$$\dot{M}_1 = \alpha_1 M_2 M_3, \qquad \dot{G}_1 = -nG_2, \tag{29}$$

$$\dot{M}_2 = \alpha_2 M_1 M_3, \qquad \dot{G}_2 = \quad n\left[1+\frac{3n}{2M^2}(2C-B-A)G_3\right]G_1, \tag{30}$$

$$\dot{M}_3 = \alpha_3 M_1 M_2, \qquad \dot{G}_3 = -\frac{3n^2}{2M^2}(2C-B-A)G_1 G_2, \tag{31}$$

where α_1, α_2 and α_3 are the following expressions

$$\alpha_1 = -\frac{C-B}{BC} - \frac{3n^2}{8M^2}(4C-3A-B), \tag{32}$$

$$\alpha_2 = \quad \frac{C-A}{AC} + \frac{3n^2}{8M^2}(4C-3B-A), \tag{33}$$

$$\alpha_3 = -\frac{B-A}{AB} + \frac{3n^2}{4M^2}(B-A). \tag{34}$$

Thus, the reduced flow lies on $\mathbb{S}^2_M \times \mathbb{S}^2_M$ and the intersections of each ball with the Hamiltonians $\mathscr{H}_M$ and $\mathscr{H}_G$ give the trajectories in the M and G spaces (see Fig. 2). As a function of the angular momentum, two main types of dynamics ought to be considered, namely: slow and fast rotations associated to small and large values of M respectively.

4.2. Relative equilibria and bifurcations

The above system of differential equations (29)-(31) has a number of equilibria related to periodic orbits in the Andoyer's angle μ (relative equilibria), the cyclic variable around which the reduction is carried out. According to Tab. 1, we classify these equilibria in three groups depending on the range of values of M where such equilibria exist, namely:

• **Permanent equilibria.** It is straightforward to verify the existence of 12 equilibria composed by combinations of the directions of the coordinate axes in the M-sphere with the two poles of G-sphere (see equilibria $E_1 - E_6$ in Tab. 1). These are called permanent equilibria because they exist for any value of M.

• **Transitory equilibria (pitchfork bifurcation).** There are other 12 sextuples of equilibria composed again by combinations of the directions of the coordinate axes in the M-sphere with two new points out of the poles of the G-sphere in the meridian $G_1 - G_3$, always at the south hemisphere of this sphere (see equilibria $E_7 - E_9$ in Tab. 1).

Indeed, apart from the poles of the G-sphere, in order to have other equilibria, the coordinate G_2 must be zero. Then, there is a particular value of the coordinate G_3 which cancels out $\dot{G}_2$ in Eq. 30, namely

$$G_3^{\mathrm{eq}} = -\frac{2M^2}{3n(2C-B-A)} < 0. \tag{35}$$

Table 1. The below sextuples of $\mathbb{S}^2_M \times \mathbb{S}^2_M$ correspond to relative equilibria for a generic triaxial body. This table is split in three parts according to the range of values of M where these equilibria exist. Thus, note that there are 12 sextuples of permanent equilibria arranged in 6 sets $E_1 - E_6$; other 12 sextuples of transitory equilibria arranged in 3 sets $E_7 - E_9$; and 4 circles of equilibria arranged in other 3 sets $E_{10} - E_{12}$. For details about of the evolution of the values of the energy for each of the equilibria given in the last column, the reader should go to Fig. 5.

Permanent equilibria			
Region	M	Equilibria	Energy
I_D	$(0,+\infty)$	$E_1 = (\pm M,0,0,0,0,M)$	H_1
I_D	$(0,+\infty)$	$E_2 = (0,\pm M,0,0,0,M)$	H_2
I_D	$(0,+\infty)$	$E_3 = (0,0,\pm M,0,0,M)$	H_3
I_D	$(0,+\infty)$	$E_4 = (\pm M,0,0,0,0,-M)$	H_4
I_D	$(0,+\infty)$	$E_5 = (0,\pm M,0,0,0,-M)$	H_5
I_D	$(0,+\infty)$	$E_6 = (0,0,\pm M,0,0,-M)$	H_6
Transitory equilibria			
Region	M	Isolated equilibria	Energy
I_D	$(0,M_C^G)$	$E_7 = (\pm M,0,0,\pm G_1^{\rm eq},0,G_3^{\rm eq})$	H_7
I_D	$(0,M_C^G)$	$E_8 = (0,\pm M,0,\pm G_1^{\rm eq},0,G_3^{\rm eq})$	H_8
I_D	$(0,M_C^G)$	$E_9 = (0,0,\pm M,\pm G_1^{\rm eq},0,G_3^{\rm eq})$	H_9
Punctual equilibria			
Region	M	Circles of equilibria	Energy
I_D	$M = M_C^M$	$E_{10} = (\pm M_1,\pm M_2,0,0,0,M_C^M)$	H_{10}
I_D	$M = M_C^M$	$E_{11} = (\pm M_1,\pm M_2,0,0,0,-M_C^M)$	H_{11}
T_2^*	$M = M_C^M < M_C^G$	$E_{12} = (\pm M_1,\pm M_2,0,\pm G_1^{\rm eq},0,G_3^{\rm eq})$	H_{12}

from where it is immediately followed that

$$G_1^{\rm eq} = \pm\sqrt{M^2-(G_3^{\rm eq})^2} = \pm M\sqrt{1-\frac{4M^2}{9n^2(2C-B-A)^2}} \tag{36}$$

giving the equilibrium point $(\pm G_1^{\rm eq}, 0, G_3^{\rm eq})$, *i.e.*, two points moving along the meridian G_1G_3.

However, note that the existence of these equilibria is restricted to be within the interval $(0, M_C^G)$, being

$$M_C^G = \frac{3n}{2}(2C-B-A) \tag{37}$$

the maximum value that M can reach for which these two points collaps at the south pole where $G_3^{\rm eq} = -M_C^G$, which is precisely the value giving the pitchfork bifurcation.

This bifurcation may be better explained by observing the evolution of the intersection between the energy parabolic cylinder ($\mathscr{H}_G$) and the rotational angular momentum sphere ($\mathbb{S}^2_M$). Indeed, reordering Eq. 28, we may express the parabolic cylinder as

$$G_3 = \frac{3n}{4M^2}(2C - B - A)G_1^2 - \mathscr{H}_G^*, \qquad \mathscr{H}_G^* = \frac{1}{n}\left[\mathscr{H}_G - \frac{n^2}{8}(2C - B - A)\right] \tag{38}$$

whose intersections with the sphere generate generic flows given in Fig. 2. More precisely, fixing a value of the radius of the M-sphere we may reduce the analysis of the dynamics to the plane $G_2 = 0$ as illustrated in Fig. 3. Note that for $M \approx 0$ we have two stable equilibria near the equator of the sphere (at the maximum circle G_1G_3), which move towards the south pole as M increases, collapsing exactly when $M = M_C^G$.

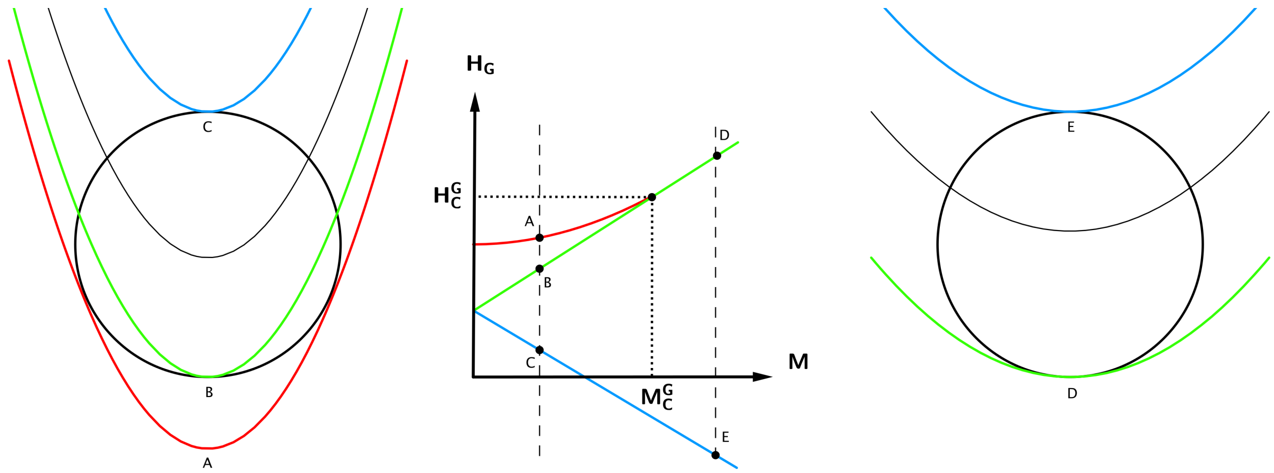

Figure 3. The reduced space G and its pitchfork bifurcation as a function of $M \leq M_C^G$. The center figure illustrates the associated energy-momentum mapping with the energy of the equilibria in this sphere.

• **Punctual equilibria.** The last group of equilibria ($E_{10} - E_{12}$ in Tab. 1) has been called punctual because they can only exist when

$$M = M_C^M = \frac{n}{2}\sqrt{3AB}, \tag{39}$$

where M_C^M is the special value for which $\alpha_3 = 0$ in Eq. 31, giving a circumference of equilibria at the equator of M-sphere when $M_3 = 0$. Note that $\alpha_1 \neq 0$ and $\alpha_2 \neq 0$ respectively in Eq. 32 and 33.

The sextuples of equilibria are given by the combination of any point at the equator of M-sphere with either the poles of the G-sphere or the aforementioned couple of equilibria at the maximum circle G_1G_3 whether the special value M_C^G has still not been reached.

Finally, the evolution of these equilibria depends also on the value of the moments of inertia. Indeed, in this case the role of triaxility is illustrated in Fig. 4, where two regions (T_1^* and T_2^*) are distinguished on the inertia plane I_D given by

$$I_D = \{A, B, C \in \mathbb{R}^+; A \leq B \leq C, A + B > C\}, \tag{40}$$

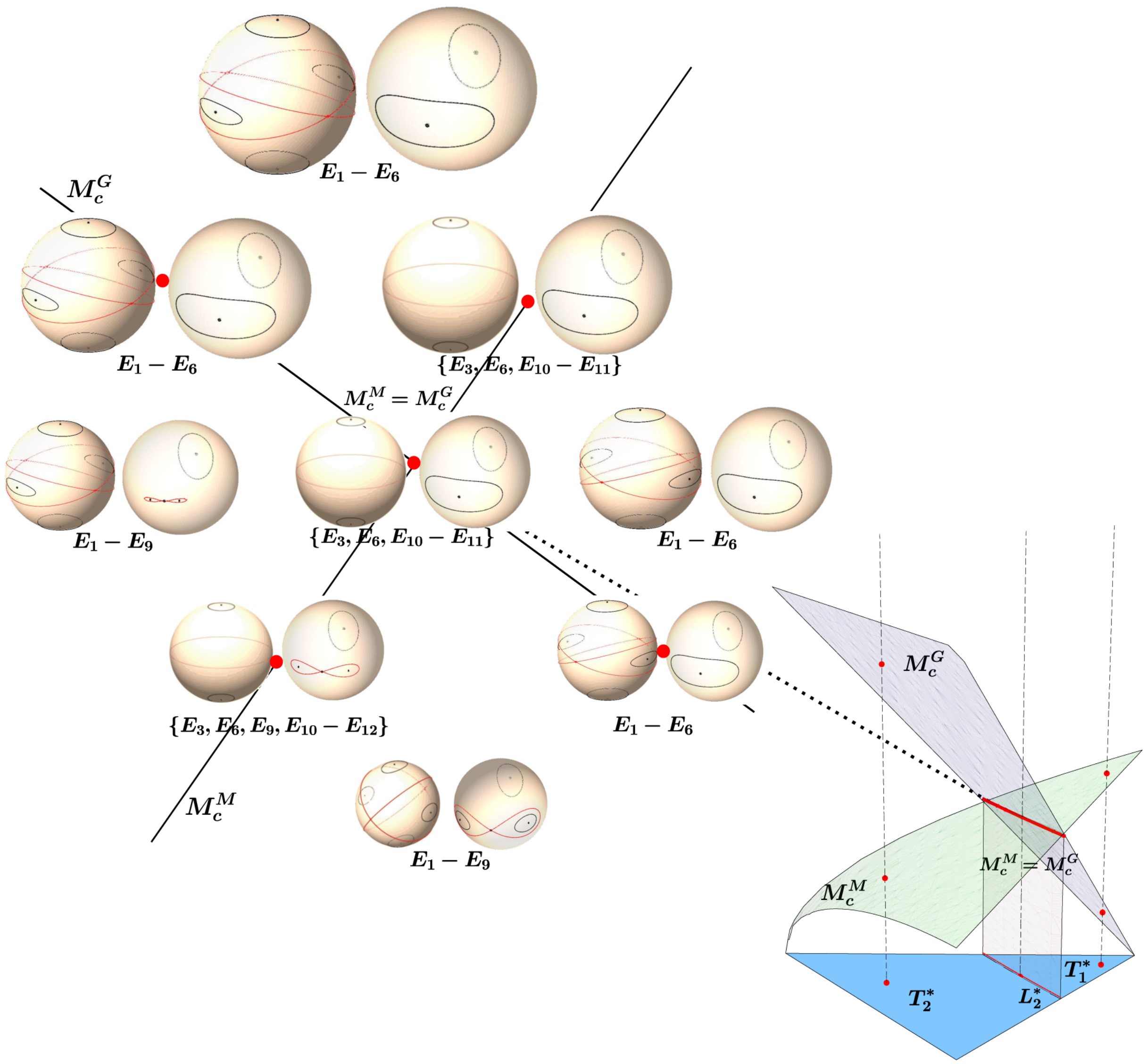

Figure 4. Evolution of flows and relative equilibria according to the value of M. Note that, for triaxial bodies, there are two regions and one curve where this evolution is different, namely: T_1^* (with $M_C^M > M_C^G$), L_2^* (with $M_C^M = M_C^G$) and T_2^* (with $M_C^M < M_C^G$). Expressions for M_C^M and M_C^G are given in Eq. 37 and 39.

which are delimited by the special curve L_2^* where $M_C^M = M_C^G$. By equating these two critical values given in Eq. 37 and 39, we find the expression for L_2^* in I_D to be

$$\frac{B}{C} = 2 - \frac{5}{6}\frac{A}{C} - \frac{1}{6}\sqrt{\frac{A}{C}\left(24 - 11\frac{A}{C}\right)} \tag{41}$$

from where we also have

$$M^*(L_2^*) = C\frac{n}{2}\sqrt{3\frac{A}{C}\left(2 - \frac{5}{6}\frac{A}{C} - \frac{1}{6}\sqrt{\frac{A}{C}\left(24 - 11\frac{A}{C}\right)}\right)} \tag{42}$$

The evolution of the whole set of equilibria may be explained from L_2^* in Fig. 4. We may observe the surfaces M_C^M and M_C^G over the inertia plane I_D, where three vertical lines (one for each region) have been traced out representing the third dimension M of the graph. The intersection of these two surfaces (curve L_2^*) generates four spatial regions plus the four boundaries among such regions whose 2D projection is given in the top-left corner of the picture. In this projection the curve L_2^* has been reduced to a point from which, by moving to any of the eight directions, the change of equilibria (bifurcations) can be observed. Note that each one of these eight regions has been labeled with their corresponding sextuples in Tab. 1.

4.3. Stability

There exist several definitions of the stability of a stationary point. We consider here the classical definition of stability in the Lyapunov's sense (see for example [24], [25]), that is, an equilibrium point E is stable if for every $\varepsilon > 0$, there is a $\delta > 0$ such that $\|E - \phi(t, X_0)\| < \varepsilon$ for all t whenever $\|E - X_0\| < \delta$, where $\phi(t, X_0)$ is the flow through X_0. The study of the linearized system also plays a role in the stability. When all eigenvalues of the linearized system have nonpositive real parts, we say that it is spectrally stable, and if the linearized system is stable at E in the above sense, we say that the original system is linearly stable.

Linear instability implies the same for the original nonlinear system. The ambiguity arises when we obtain linear and/or spectral stability. This case may be tackled by means of the Energy-Casimir method, see [17]. In our study, we combine both approaches as well as we take advantage from the fact that the flow may be projected and visualized in the M and G spaces. Figure 5 summarizes the parametric dependency study of the stability in the plane M, G. For details, see [11].

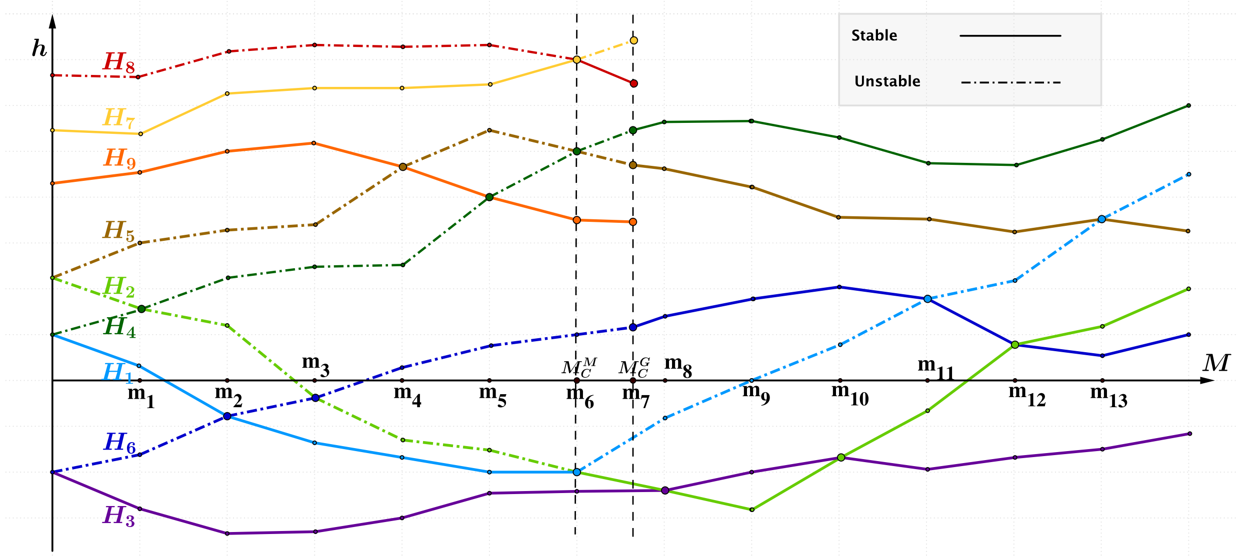

Figure 5. Energy-Momentum map for region T_1^*: Each polygonal line represents, qualitatively, the energy of an equilibria. Tick-marks in the M-axis are placed for each intersection of the energy curves. The regions in M where the equilibria are stable correspond with continuous lines, the dashed line is used for unstable equilibria. Note that the scale has been modified.

5. Intermediary $\mathscr{H}_\nu$

The Hamiltonian of the intermediary $\mathscr{H}_\nu$ is studied in [8], where it is shown that , in the rotating frame, it may be put into the following form by taking into account Eq. (15) and Eq. (16),

$$\begin{aligned}\mathscr{H}_\nu \equiv \mathscr{H}_0^\nu &= \frac{1}{2}\left(\frac{\sin^2\nu}{A}+\frac{\cos^2\nu}{B}\right)(M^2-N^2)+\frac{N^2}{2C}-n\Phi \\ &+n^2\Delta\left[\left(\frac{2}{3}-\sin^2 I\right)\left(\frac{2}{3}-\sin^2 J\right)+f_3\left(\frac{2}{3}-\sin^2 I\right)\sin^2 J\cos 2\nu\right]\end{aligned} \tag{43}$$

where we have used the notations introduced by Kinoshita and Andoyer

$$\frac{1}{D}=\frac{1}{C}-\frac{1}{2}\left(\frac{1}{A}+\frac{1}{B}\right), \qquad \chi=\frac{C(B-A)}{C(A+B)-2AB} \tag{44}$$

together with

$$f_3=\frac{B-A}{2C-B-A}>0, \qquad \Delta=-\frac{9}{16}(2C-B-A)<0, \tag{45}$$

5.1. The reduced space. From Hamiltonian to Poisson dynamics

Proceeding in the same way that in the case of the intermediary $\mathscr{H}_{\{\nu,\phi\}}$, we apply the non-symplectic transformation from Andoyer to the MG-space, which leads us to the Hamiltonian

$$\mathscr{H}_0^\nu=\frac{1}{2}\left(\frac{M_1^2}{A^*}+\frac{M_2^2}{B^*}+\frac{M_3^2}{C^*}\right)-nG_3-\frac{n^2}{8}(A+B+C)\left(1-3\frac{G_3^2}{M^2}\right). \tag{46}$$

where

$$\frac{1}{A^*}=\frac{1}{A}+n^2\frac{3A}{4M^2}\left(1-\frac{3G_3^2}{M^2}\right), \quad \frac{1}{B^*}=\frac{1}{B}+n^2\frac{3B}{4M^2}\left(1-\frac{3G_3^2}{M^2}\right), \quad \frac{1}{C^*}=\frac{1}{C}+n^2\frac{3C}{4M^2}\left(1-\frac{3G_3^2}{M^2}\right) \tag{47}$$

On the other side, the system of differential equations associated to Eq. (46) is given by

$$\dot{M}_1=a_1M_2M_3, \qquad \dot{G}_1=-\Delta(M_i)G_2, \tag{48}$$

$$\dot{M}_2=a_2M_1M_3, \qquad \dot{G}_2=\Delta(M_i)G_1, \tag{49}$$

$$\dot{M}_3=a_3M_1M_2, \qquad \dot{G}_3=0. \tag{50}$$

where

$$a_1=-\frac{C-B}{4BCM^4}[4M^4-3BCn^2(M^2-3G_3^2)], \tag{51}$$

$$a_2=\frac{C-A}{4ACM^4}[4M^4-3ACn^2(M^2-3G_3^2)], \tag{52}$$

$$a_3=-\frac{B-A}{4ABM^4}[4M^4-3ABn^2(M^2-3G_3^2)], \tag{53}$$

and

$$\Delta(M_i) = \frac{n}{4M^4}\{4M^4 + 3G_3n[3(AM_1^2 + BM_2^2 + CM_3^2) - M^2(A+B+C)]\}. \qquad (54)$$

Note that the previous equations define two coupled subsystems. The system $\dot{M}_i$ is an Euler-type system, meanwhile $\dot{G}_i$ defines a non-autonomous Hamiltonian given by

$$\mathscr{H}(G_i) = \frac{1}{2}\Delta(M_i)(G_1^2 + G_2^2) \qquad (55)$$

5.2. Relative equilibria and bifurcations

The study of the relative equilibria of this system is influenced by the moments of inertia, which are located in different regions of the parameter plane as in the previous model. More precisely among the valid terns in the domain I_D (see Fig. 6) we distinguish the oblate symmetric bodies given by $L_1 = \{(A,B,C) \in D : A/C = B/C\}$, the prolate symmetric bodies $L_3 = \{(A,B,C) \in D : A = B\}$, and the flat bodies L_4. Finally we consider the generic triaxial cases $T_1 = \{(A,B,C) \in D : 2B < A + C\}$, $T_2 = \{(A,B,C) \in D : 2B > A + C\}$ and the special one $L_2 = \{(A,B,C) \in D : 2B = A + C\}$.

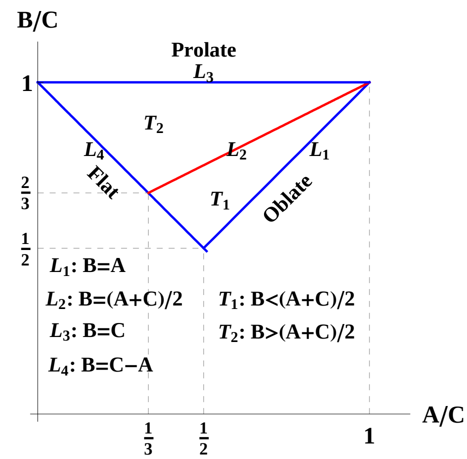

Figure 6. Triaxiality domains. The red line L_2 separating the regions T_1 and T_2 requieres a particular analysis since some expressions are not defined for this values.

A large number of the equilibria and their bifurcations hinges on the domain of the moments of inertia. In Fig. 7 we present the configurations of the bifurcations lines of the equilibria depending on the particular region of the triaxiality domain in which the moments of inertia lie.

The whole scenario of equilibria is summarized in Tab. 2, where we have classified those equilibria in two groups depending on the range of values of M and the triaxiality domain region where the moments of inertia belong.

• **Permanent equilibria**. Their existence is straightforward to verify by simply substitution in the differential system (48)-(50), (see equilibria E_1-E_6 in Tab. 2). Those equilibria do not depend on the triaxiality domain nor in the value of M, thus we have called them permanent.

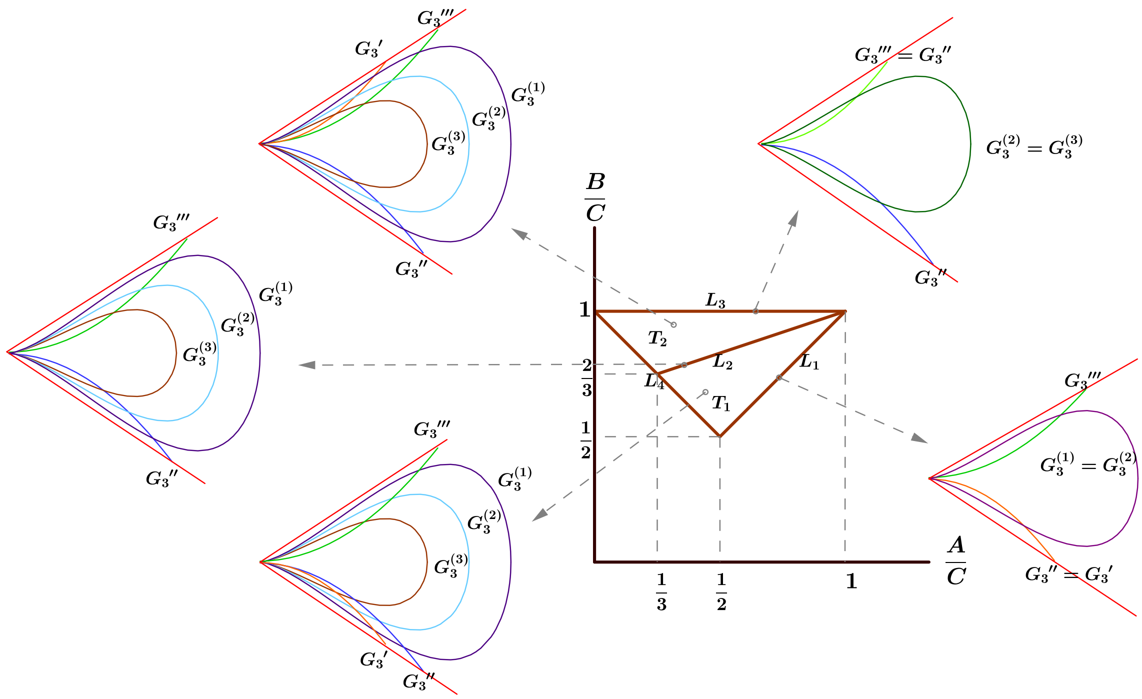

Figure 7. Different momentum-momentum planes over the triaxility domain. The different curves are related to bifurcations of the previous equilibria.

• **Other equilibria**. They correspond to equilibria that exists on particular range of M and triaxility regions, see equilibria E_7-E_{20} in Tab. 2. The equilibria E_7-E_9 correspond with the principal direction in the M-space and a particular value of G_3 that make $\Delta(M)$ vanishes. From $E_1$0-$E_2$0 we obtain equilibria that are located in the coordinate planes of the M-space but do not correspond with the usual equilibria of the rigid body in the coordinate axes.

Next we study in detail the equilibria and their bifurcations for the case that the triaxiality belongs to T_2. Curves where we find relative equilibria of the system Eqs. (48)-(50) in the space $G_3 - M$ are shown in Fig. 8. Firstly on the lines $G_3 = \pm M$ we have the E_1-E_6 relative equilibria. We also have the curves G_3' (blue), G_3'' (orange) and G_3''' (green) standing for circumferences on the G_3-sphere whose combination with the directions of the coordinates axes of the M-sphere give the E_7-E_9 relative equilibria. Finally the curves $a_1 = 0$ (purple), $a_2 = 0$ (cyan) and $a_3 = 0$ (brown) host the E_{10}-E_{20} equilibria.

In short, the analysis of this intermediary in a rotating frame shows the existence of several relative equilibria for small values of the rotational angular momentum. They depend on the moments of inertia within different regions of the parameter plane (Figure 6). Note that these equilibria highlights some remarkable differences between this intermediary and the Euler-Poinsot motion. Moreover, the addition of a perturbing potential makes it possible to find conditions where $\dot{\mu} = 0$, which is not possible when dealing with the free rigid body motion. This potential has a further

Table 2. The below initial conditions correspond to equilibria for a general body. This table is split in two parts, the first one does not assume any condition on the value of the integrals and the second one hinges on a set of special values of them. Expressions corresponding to labels are given in [11].

Permanent equilibria		
Region	M	Equilibria
I_D	$(0,+\infty)$	$E_1=(\pm M,0,0,0,0,M)$
I_D	$(0,+\infty)$	$E_2=(0,\pm M,0,0,0,M)$
I_D	$(0,+\infty)$	$E_3=(0,0,\pm M,0,0,M)$
I_D	$(0,+\infty)$	$E_4=(\pm M,0,0,0,0,-M)$
I_D	$(0,+\infty)$	$E_5=(0,\pm M,0,0,0,-M)$
I_D	$(0,+\infty)$	$E_6=(0,0,\pm M,0,0,-M)$
Other equilibria		
Region	M	Equilibria
I_D	$(0,\mathscr{M}')$	$E_7=(\pm M,0,0,G_1,G_2,G_3')$
I_D	$(0,\mathscr{M}'')$	$E_8=(0,\pm M,0,G_1,G_2,G_3'')$
I_D	$(0,\mathscr{M}''')$	$E_9=(0,0,\pm M,G_1,G_2,G_3''')$
T_1	$(0,\mathscr{M}_1^{(2)})$	$E_{10}=(0,\pm M_2^{(1)},\pm M_3^{(1)},G_1,G_2,G_3^{(1)})$
T_1	$(0,\mathscr{M}_1^{(1)})$	$E_{11}=(0,\pm M_2^{(1)},\pm M_3^{(1)},G_1,G_2,-G_3^{(1)})$
T_2	$(\mathscr{M}_1^{(1)},\mathscr{M}_1^{(2)})$	$E_{12}=(0,\pm M_2^{(1)},\pm M_3^{(1)},G_1,G_2,G_3^{(1)})$
I_D	$(0,\mathscr{M}_2^{(2)})$	$E_{13}=(\pm M_1^{(2)},0,\pm M_3^{(2)},G_1,G_2,G_3^{(2)})$
I_D	$(0,\mathscr{M}_2^{(1)})$	$E_{14}=(\pm M_1^{(2)},0,\pm M_2^{(2)},G_1,G_2,-G_3^{(2)})$
T_1	$(0,\mathscr{M}_3^{(1)})$	$E_{15}=(\pm M_1^{(3)},\pm M_2^{(3)},0,G_1,G_2,G_3^{(3)})$
T_2	$(0,\mathscr{M}_3^{(2)})$	$E_{16}=(\pm M_1^{(3)},\pm M_2^{(3)},0,G_1,G_2,-G_3^{(3)})$
T_1	$(\mathscr{M}_3^{(1)},\mathscr{M}_3^{(2)})$	$E_{17}=(\pm M_1^{(3)},\pm M_2^{(3)},0,G_1,G_2,-G_3^{(3)})$
L_2	$(0,\mathscr{M}_1^{(2)})$	$E_{18}=(\pm M,0,0,G_1,G_2,G_3^{(1)})$
L_2	$(0,\mathscr{M}_3^{(2)})$	$E_{19}=(\pm M_1^{(3)},\pm M_2^{(3)},0,G_1,G_2,G_3^{(3)})$
L_2	$(0,\mathscr{M}_3^{(2)})$	$E_{20}=(\pm M_1^{(3)},\pm M_2^{(3)},0,G_1,G_2,-G_3^{(3)})$

effect related to the stability of relative equilibria over the $M-$sphere. Indeed, there is a change of position of the unstable equilibria associated with the torque-free motion; expressions show the dependency on the values of the momenta M and G_3 and the moments of inertia. A comprehensive study giving the whole set of formulas will be published elsewhere[11].

5.3. Stability

For the study of the stability we follow the same approach than in the previous intermediary. In this case, the set of equilibria dubbed as other equilibria are easily classified as unstable, since the flow in the G-space is made of circles at G_3 constant. Therefore, it make sense to perform the second reduction and study the stability in the M-space. As we have a rigid body flow type in the M-space, the stability of the equilibria corresponds with two stable equilibria and one unstable. Nevertheless, as we move by the different regions in the G_3-M plane at a fixed G_3, the stability of the equilibria interchanges between each other (see Fig. 9).

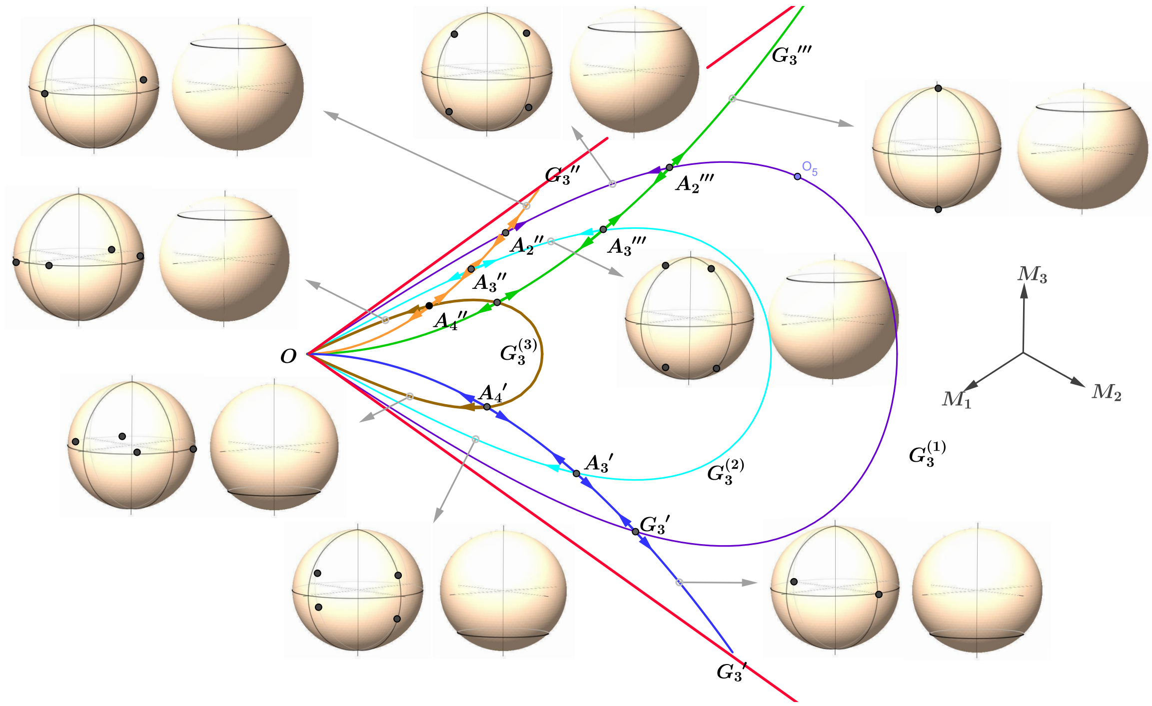

Figure 8. The MG_3-plane showing the curves where relative equilibria and bifurcations are found for the T_2 region.

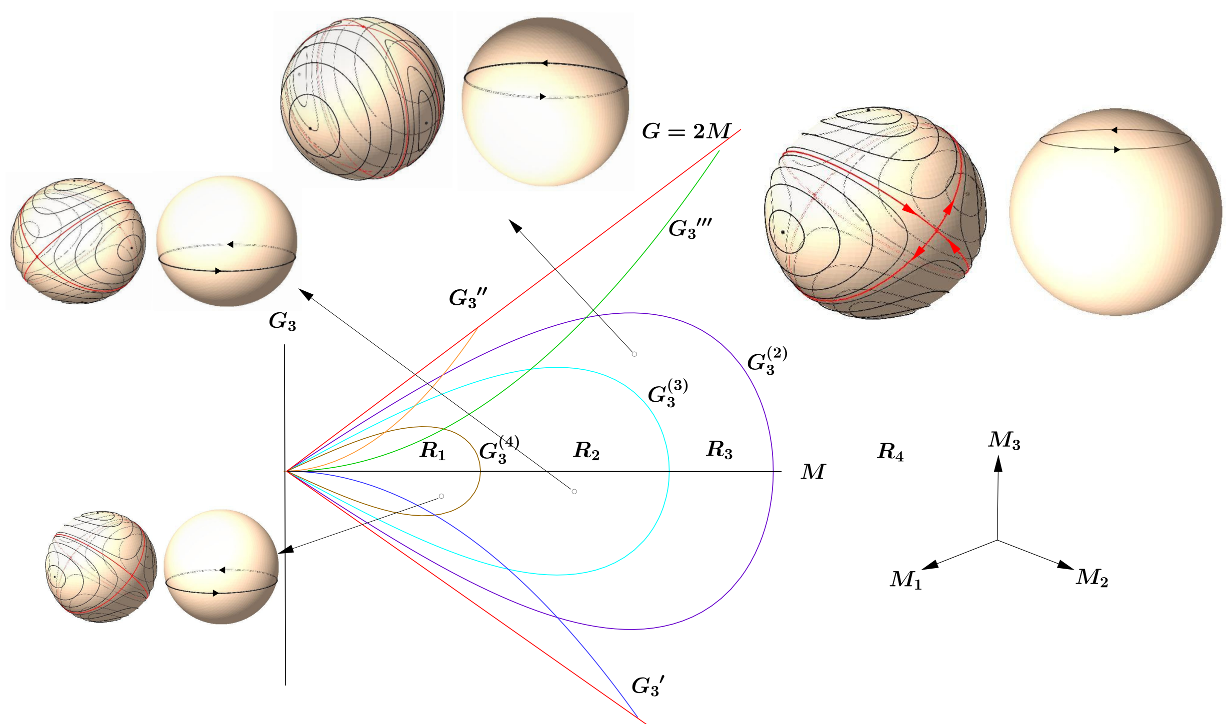

Figure 9. Different dynamics over the MG_3-plane. Note the changes of the position of the unstable equilibria in the M-sphere as we move in the MG_3-plane through the lines G_3^2, G_3^3 and G_3^4.

6. Comparisons

In this paper we have studied two 1-DOF integrable systems. They represent approximations of the full gravity-gradient system, which is a 3-DOF with several parameters. As the reader is aware of, comparison among these systems is a task which is out of the scope of the present work. The content of this paper, nonetheless, has set up a frame in order to do those comparisons. Having stated that, we finish the paper showing some preliminary simulations. Figure 10 shows the absolute value of the maximum difference, for each variable, between the full gravity-gradient problem and the two intermediary models for three different bodies up to one revolution in the orbit. These simulations have been carried out for different inclinations of the rotational angular momentum plane with respect to reference frame. The results show that, for near-axial bodies (Fig. 10(a)), both intermediaries behave similarly. When a bit more triaxial body is considered (Fig. 10(b)), the intermediary $\mathscr{H}_\nu$ behaves clearly better than $\mathscr{H}_{\{\nu,\phi\}}$ for the angles ν and μ, giving similar performances for the rest of the variables. Same functionality is observed in Fig. 10(c) as in Fig. 10(b). Nevertheless, it is important to note again that, as these are preliminary simulations, these conclusions are still an open issue.

Acknowledgements

Support from the Government of Spain is acknowledged. It came in the form of research project MTM 2012-31883 of the Ministry of Science, and project 12006/PI/09 from Fundación Séneca of the Autonomous Region of Murcia.

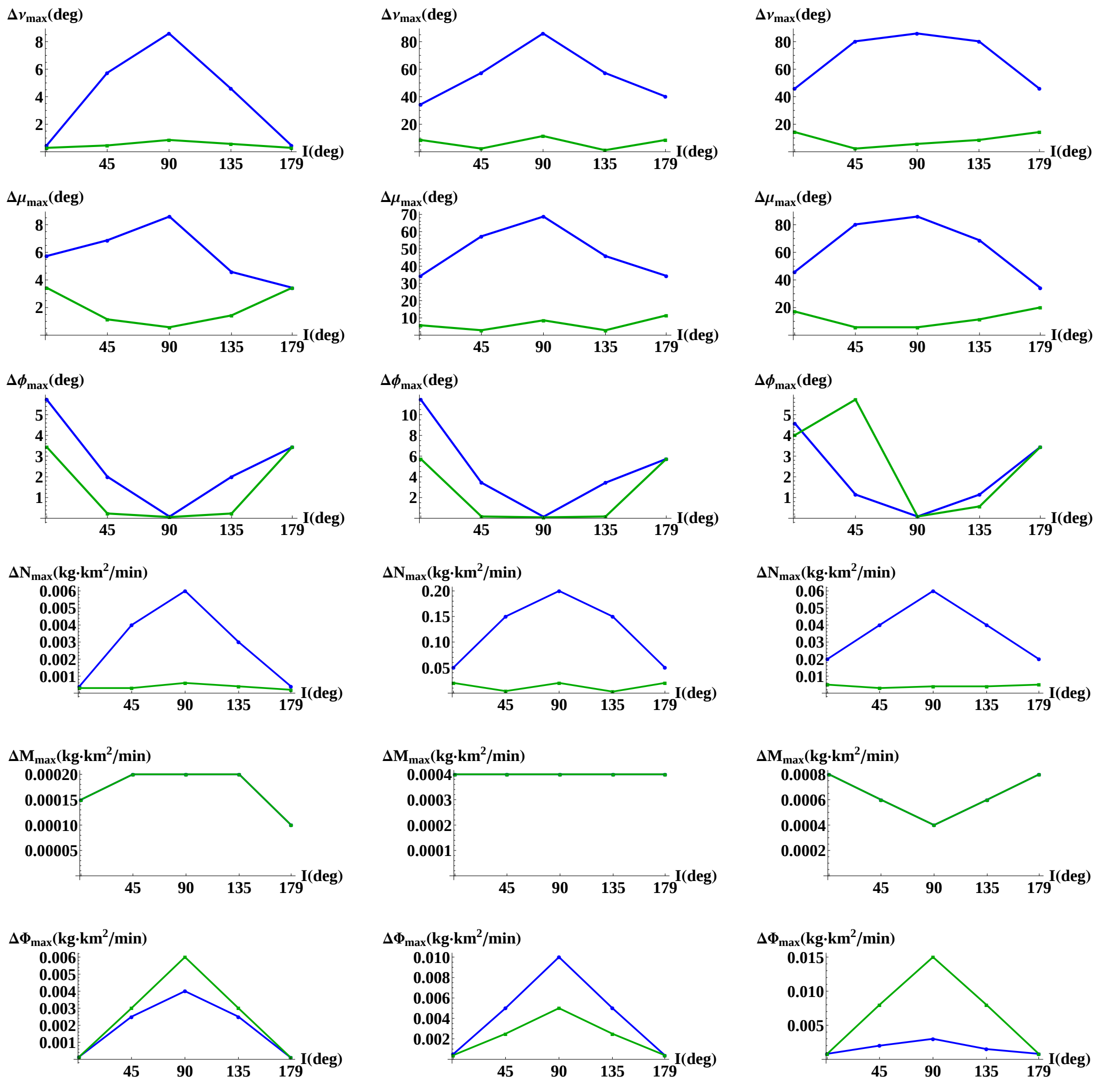

(a) $A \approx B$ (b) $A < B$ (c) $A << B$

Figure 10. Absolute value of the maximum difference, for each variable, between the full gravity-gradient problem and the two intermediary models: $\mathscr{H}_{\{\nu,\phi\}}$ (blue curve), $\mathscr{H}_{\nu}$ (green curve) for three different bodies up to one revolution in the orbit. (a) $\{A,B,C\} = \{0.28, 0.31, 0.39\}$ $(\mathrm{kg} \cdot \mathrm{km}^2)$. (b) $\{A,B,C\} = \{0.2, 0.31, 0.39\}$ $(\mathrm{kg} \cdot \mathrm{km}^2)$. (c) $\{A,B,C\} = \{0.1, 0.31, 0.39\}$ $(\mathrm{kg} \cdot \mathrm{km}^2)$.

7. References

[1] Deprit, A. “The elimination of the parallax in satellite theory.” Celestial Mechanics, Vol. 24, No. 2, pp. 111–153, 1981.

[2] Beletskii, V. V. Motion of an artificial satellite about the center of mass. Israel Prog. for Scientific Trans., Jerusalem, 1966.

[3] Scheeres, D. Orbital Motion in Strongly Perturbed Environments: Application to Asteroid, Comet and Planetary Satellite Orbiters. Jointly published with Praxis Publishing, UK, 2012.

[4] Hughes, P. C. Spacecraft Attitude Dynamics. Dover Public Inc, New York, 1986.

[5] Zanardi, M., Silva, W., Formiga, J., Stuchi, T., and Cabette, R. "Stability analysis of the spacecraft attitude with canonical variables." Proceedings of the 23$^{\text{th}}$ International Symposium on Space Flight Dynamics — 23$^{\text{th}}$ ISSFD. Pasadena, USA, 2013.

[6] Andoyer, M. H. Cours de Mécanique Céleste. Gauthier-Villars, Paris, 1923.

[7] Ferrer, S. and Lara, M. "On Roto-Translatory Motion: Reductions and Radial Intermediaries." The Journal of the Astronautical Sciences, Vol. 59, No. 1-2, pp. 22–40, 2014.

[8] Ferrer, S. and Molero. "Intermediaries for Gravity-Gradient Attitude Dynamics I. Action-angle variables." To appear in Advances in the Astronautical Sciences, 2nd IAA Conference on Dynamics and Control of Space Systems. Roma. Italy. 24-26 March 2014.

[9] Ferrándiz, J. M. and Sansaturio, M. E. "Elimination of the nodes when the satellite is a non spherical rigid body." Celestial Mechanics, Vol. 46, pp. 307–320, 1989.

[10] Arribas, M. Sobre la dinámica de actitud de satélites artificiales. PhD, Universidad de Zaragoza, 1989.

[11] Ferrer, S., Crespo, F., Molero, F. J., and van der Meer, J. C. "A gravity-gradient intermediary in attitude dynamics. Relative equilibria and bifurcations." 10th AIMS Conference on Dynamical Systems, Differential Equations and Applications. Madrid, Spain, 7-11 July, 2014.

[12] Ferrer, S. and Molero, F. J. "Andoyer variables and phases in the free rigid body." Journal of Geometric Mechanics, Vol. 6, No. 1, pp. 25–37, 2014.

[13] MacCullagh, J. "On the rotation of a solid body." Proceedings of the Royal Irish Academy, Vol. 2, pp. 520–545, 1840.

[14] Crespo, F. Hopf fibration reduction of a quartic model. An application to rotational and orbital dynamics. PhD Thesis, Universidad de Murcia, In preparation, 2014.

[15] Ferrer, S., Molero, F. J., and Crespo, F. "Intermediaries for Roto-Orbital Dynamics under Gravity-Gradient Torque. The influence of excentricity." In preparation, 2014.

[16] Abraham, R. and Marsden, J. Foundations of Mechanics. American Mathematical Society, 2nd edn., 1985.

[17] Marsden, J. and Ratiu, T. Introduction to mechanics and symmetry. Springer-Verlag New York, Inc., 2nd edn., 1999.

[18] Ortega, J. and Ratiu, T. Momentum maps and Hamiltonian reduction. Birkhuser, 2004.

[19] Cushman, R. "Reduction, Brouwers Hamiltonian, and the critical inclination." Celestial Mechanics, Vol. 31, pp. 401–429, 1983.

[20] Deprit, A. "Dynamics of orbiting dust under radiation pressure." Big-Bang Cosmology Symposium in honour of G. Lemaitre, Vol. 31, pp. 151–180, 1984.

[21] Coffey, S., Deprit, A., and Miller, B. "The critical inclination in artificial satellite theory." Celestial Mechanics, Vol. 39, pp. 365–406, 1986.

[22] Palacián, J., Sayas, F., and Yanguas, P. "Regular and Singular Reductions in the Spatial Three-Body Problem." Qualitative Theory of Dynamical Systems, Vol. 12, pp. 143–182, 2013.

[23] Hanßmann, H. Quasi-periodic Motions of a Rigid Body. A case study on perturbations of superintegrable systems. PhD, University of Groningen, 1995.

[24] Hirsch, M. and Smale, S. Differential equations, dynamical systems and linear algebra. Academic Press, Inc. San Diego, California, 1974.

[25] Arnold, V. Ordinary differential equations. The MIT press, 1973.